Inorg. Chem. **2005**, *44*, 5826–5832

Inorganic Chemistry
Article

Diphosphacarbollide Analogues of the $C_5H_5^-$ Anion: Isolation of the *nido*-Di- and Triphosphacarboranes 7,8,9-$P_2CB_8H_{10}$, [7,8,9-$P_2CB_8H_9$]$^-$, [7,8,10-$P_2CB_8H_9$]$^-$, and 7,8,9,10-$P_3CB_7H_8$

Mario Bakardjiev,[†] Josef Holub,[†] Bohumil Štíbr,[*,†] Drahomír Hnyk,[†] and Bernd Wrackmeyer[‡]

Contribution from the Institute of Inorganic Chemistry, Academy of Sciences of the Czech Republic, 250 68 Řež, Czech Republic, and Laboratorium für Anorganische Chemie der Universität Bayreuth, Postfach 101251, Bayreuth, D-95440, Germany

Received December 16, 2004

Treatment of a solution of excess PCl_3 and PS (PS = "proton sponge" = 1,8-dimethylamino naphthalene) with *arachno*-4-CB_8H_{14} (**1**) in CH_2Cl_2, followed by hydrolysis of the reaction mixture, resulted in the isolation of the eleven-vertex diphosphacarbaborane *nido*-7,8,9-$P_2CB_8H_{10}$ (**2**) (yield 34%) as the main product. Other products isolated from this reaction were the phosphacarboranes *nido*-7,8,9,10-$P_3CB_7H_8$ (**3**) (yield 5%) and *closo*-2,1-PCB_8H_9 (**4**) (yield 15%). Compound **2** can be deprotonated by PS in CH_2Cl_2 or NaH in diethyl ether to give the [*nido*-7,8,9-$P_2CB_8H_9$]$^-$ (**2**$^-$) anion, which gives back the original compound, **2**, upon re-protonation. Thermal rearrangement of anion **2**$^-$ (Na^+ salt) at 350 °C for 2 h produced the isomeric [*nido*-7,8,10-$P_2CB_8H_9$]$^-$ (**5**$^-$) anion, which was isolated as a PPh_4^+ salt (yield 86%). Multinuclear (^1H, ^{11}B, ^{31}P, and ^{13}C), two-dimensional [^{11}B–^{11}B] COSY, ^1H-{^{11}B(selective)}, ^1H{^{31}P(selective)}, and gradient-enhanced ([^1H–^{13}C] HSQC) magnetic resonance measurements led to complete assignments of all resonances which are in excellent agreement with the structures proposed. Coupling constants, $^1J(^{31}P,^{13}C)$, $^2J(^{31}P,C,^1H)$, and $^1J(^{31}P,^{31}P)$, were calculated using the DFT method B3LYP/6-311+G(d,p). The molecular geometries of all compounds were optimized ab initio at a correlated level of theory (RMP2(fc)) using the 6-31G* basis set, and their correctness was assessed by comparison of the experimental ^{11}B and ^{13}C chemical shifts with those calculated by the GIAO–SCF/II//RMP2(fc)/6-31G* method. The computations also include the structures and chemical shieldings of the still unknown isomers [*nido*-7,10,8-$P_2CB_8H_9$]$^-$ (**6**$^-$) and [*nido*-7,9,8-$P_2CB_8H_9$]$^-$ (**7**$^-$).

Introduction

There is current interest in the synthesis and chemistry of the eleven-vertex nido phosphacarboranes because of their high stability and interesting chemical behavior, specifically metal complexation.[1] Todd et al. pioneered this area by the characterization of the phosphamonocarbaborane anion [7,8-PCB_9H_{11}]$^-$.[2] Formal replacement of one BH^- group in [PCB_9H_{11}]$^-$ with the isolobal CH vertex leads to the phosphadicarbaborane series $PC_2B_8H_{11}$, for which the synthesis of compounds 7,8,11-$PC_2B_8H_{11}$ and [7,8,11-$PC_2B_8H_{10}$]$^-$, along with the preparation of the isomeric species 7,8,9-$PC_2B_8H_{11}$ and [7,8,9-$PC_2B_8H_{10}$]$^-$, have been reported.[3,4] Sneddon and co-workers have also prepared neutral compounds 7-R-7,8,9-$PC_2B_8H_{10}$ (R = Me and Ph)[5] substituted on the cluster phosphorus atom. Further isolobal CH → P considerations in the eleven-vertex nido series lead to the neutral $P_2C_2B_7H_9$ and $P_3CB_7H_8$ compounds. These are represented by the three 7,8,9,11-, 7,9,8,10-, and 7,8,9,10-$P_2C_2B_7H_9$ isomers[6] and substituted derivatives of 7,8,9,10-$P_3CB_7H_8$.[7] The eleven-vertex nido diphopsphamonocarbab-

---

[*] To whom correspondence should be addressed. E-mail: stibr@iic.cas.cz.

[†] Intstitute of Inorganic Chemistry.

[‡] Laboratorium für Anorganische Chemie.

(1) See, for example: (a) Todd, L. J.; Paul, I. C.; Little, J. L.; Welcker, P. S.; Peterson, C. R. *J. Am. Chem. Soc.* **1968**, *90*, 4489. (b) Štíbr, B.; Holub, J.; Bakardjiev, M.; Pavlík, I.; Tok, O. L.; Císařová, I.; Wrackmeyer, B.; Herberhold, M. *Chem.—Eur. J.* **2003**, 2239. (c) Štíbr, B.; Holub, J.; Bakardjiev, M.; Pavlík, I.; Tok, O. L.; Wrackmeyer, B. *Eur. J. Inorg. Chem.* **2003**, 2524.

(2) (a) Todd, L. J.; Paul, I. C.; Little, J. L.; Welcker, P. S.; Peterson, C. R. *J. Am. Chem. Soc.* **1968**, *90*, 4489. (b) Todd, L. J.; Little, J. L.; Silverstein, H. T. *Inorg. Chem.* **1969**, *8*, 1698.

(3) Holub, J.; Ormsby, D. L.; Kennedy, J. D.; Greatrex, R.; Štíbr, B. *Inorg. Chem. Commun.* **2000**, *3*, 178.

(4) Štíbr, B.; Holub, J.; Bakardjiev, M.; Hnyk, D.; Tok, O. L.; Milius, W.; Wrackmeyer, B. *Eur. J. Inorg. Chem.* **2002**, 2320.

(5) Shedlow, M.; Sneddon, L. G. *Inorg. Chem.* **1998**, *37*, 5269.

10.1021/ic048232c CCC: $30.25

Scheme 1. Phosphacarboranes from *arachno*-4-CB_8H_{14} (**1**)[a]

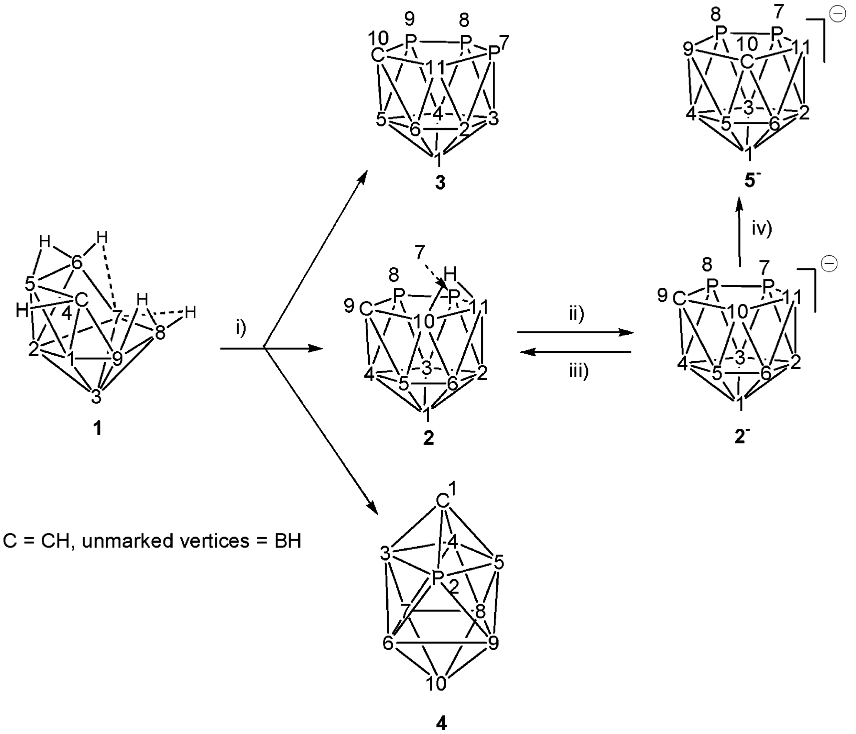

[a] (i) PCl_3, PS, 12 h, room temperature; (ii) PS in MeCN or NaH in Et_2O, room temperature; (iii) H_2SO_4, CH_2Cl_2, 0 °C; and (iv) Na^+ salt, 2 h, 350 °C.

oranes, $P_2CB_8H_{10}$, and tricarbaphosphaboranes, $PC_3B_7H_{10}$, have remained unknown. We report here the synthesis of the first representatives of the diphopsphamonocarbaborane family, compounds 7,8,9-$P_2CB_8H_{10}$, [7,8,9-$P_2CB_8H_9$]$^-$, and [7,8,10-$P_2CB_8H_9$]$^-$, together with the yet unknown parent 7,8,9,10-$P_3CB_7H_8$ species.

Results and Discussion

Syntheses. As shown in Scheme 1, a CH_2Cl_2 solution containing an excess of PCl_3 and PS was treated with a solution of *arachno*-4-CB_8H_{14} (**1**) at ambient temperature for 12 h (path i). After hydrolysis and chromatographic separation of the products, the neutral compound **2** was isolated as a predominant product (yield 34%) along with the triphosphacarbaundecaborane *nido*-7,8,9,10-$P_3CB_7H_8$ (**3**) (yield 5%) and, the previously reported,[8] phosphacarborane *closo*-2,1-PCB_8H_9 (**4**) (yield 15%). As inferred from Scheme 1, the main reaction mode, characterized by the formation of compound **2**, is consistent with the insertion of two adjacent phosphorus vertexes into the area identified by the C4, B5, B6, B7, B8, and B9 vertexes in the open hexagonal face of carborane **1**. Compound **3**, then, seems to be generated by removing the B6 vertex from *arachno* compound **1** and inserting three P atoms along the open face of the remaining CB7 fragment.

Neutral *nido*-7,8,9-$P_2CB_8H_{10}$ compound **2** can be deprotonated either by PS or NaH to give the [*nido*-7,8,9-$P_2CB_8H_9$]$^-$ anion **2**$^-$ (path ii), which gives back the original compound, **2**, upon re-protonation (path iii). Anion **2**$^-$ was finally characterized as PPh_4^+ and PSH^+ salts (yields 93 and 92%, respectively). Thermal rearrangement of Na^+[*nido*-7,8,9-$P_2CB_8H_9$]$^-$ (Na^+**2**$^-$), effected by heating at 350 °C for 2 h (path iv), followed by precipitation with PPh_4Cl in water, resulted in the isolation of the isomeric species PPh_4^+[*nido*-7,8,10-$P_2CB_8H_9$]$^-$ (PPh_4^+**5**$^-$) in a yield of 86%. The net result of the isomerization is the migration of the C9 vertex into the C10 position. The reaction is very clean and no P-migration mode, which would lead to [*nido*-7,10,8-P_2-CB_8H_9]$^-$ (**6**$^-$), was observed. The proposed mechanism for the **2**$^-$ → **5**$^-$ rearrangement process is outlined in Scheme 2 and is essentially based on the one reported earlier by Sneddon et al. for a similar rearrangement in the C-substituted eleven-vertex nido tricarbaborane series.[9] Scheme 2 shows that a B10 migration (path i) in **2**$^-$, followed by C (path ii), and B8 (path iii) migrations in the open face, finally leads to stable C_s symmetry with all three heteroatoms in the open face as in **5**$^-$. This type of isomerization is entirely analogous to the [7,8,9-$C_3B_8H_{11}$]$^-$ → [7,8,10-$C_3B_8H_{11}$]$^-$ rearrangement earlier reported by one of our groups.[10]

Geometry Optimization. Although we have been able to grow good crystals of all of the compounds, **2**, **2**$^-$, **3**, and **5**$^-$, the corresponding X-ray diffraction experiments suffered, typically, from the extensive disorder of the P vertexes. The

---

(6) Holub, J.; Jelínek, T.; Hnyk, D.; Plzák, Z.; Císařová, I.; Bakardjiev, M.; Štíbr, B. *Chem.—Eur. J.* **2001**, *7*, 1546.

(7) Jelínek, T.; Hnyk, D.; Holub, J.; Štíbr, B. *Inorg. Chem.* **2001**, *40*, 4512.

(8) Holub, J.; Bakardjiev, M.; Štíbr, B.; Hnyk, D.; Tok, O. L.; Wrackmeyer, B. *Inorg.Chem*. **2002**, *41*, 2817.

(9) Wille, A. E.; Sneddon, L. G. *Collect. Czech. Chem. Commun*. **1997**, *62*, 1214.

(10) (a) Štíbr, B.; Holub, J.; Císařová, I.; Teixidor, F.; Viñas, C. *Inorg. Chim. Acta*, **1996**, *245*, 129. (b) Holub, J.; Štíbr, B.; Hnyk, D.; Fusek, J.; Císařová, I.; Teixidor, F.; Viñas, C.; Plzák, Z.; Schleyer, P. v. R. *J. Am. Chem. Soc*. **1997**, *119*, 7750.

Scheme 2. Proposed Mechanism for the Rearrangement of [*nido*-7,8,9-$P_2CB_8H_9$]− (**2**−) into [*nido*-7,8,10-$P_2CB_8H_9$]− (**5**−) via the Migration of the B and C vertexes[a]

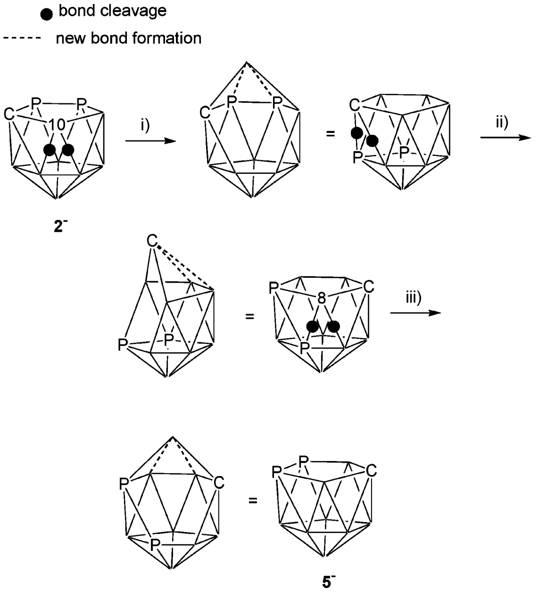

[a] (i) B10 migration; (ii) C migration; and (iii) B8 migration.

geometry of compound **4** was reported sufficiently in a preliminary communication,[7] while those of compounds **2**, **2**$^-$, **3**, and **5**$^-$ were optimized at the RMP2(fc)/6-31G* level, as the final level of optimization. These geometries were used for GIAO−SCF/II//RMP2(fc)/6-31G* calculations of the ^{11}B and ^{13}C NMR chemical shifts. Comparisons of calculated shifts with experimental values reveal satisfactory agreement (maximum difference for δ (^{11}B) range was 4 ppm). The δ (^{13}C) calculations performed slightly worse but these usually show strong dependence on the theory and basis set used.[11] Nevetheless, the calculations provide a good ground for believing that the RMP2(fc)/6-31G* internal coordinates can be deemed as good representations of the molecular geometries for all of the compounds under study in their solutions. The calculated geometries are depicted in Figure 1, and Table 1 shows the computed geometrical parameters. Apparently, the presence of the two or three phosphorus vertexes is a principal source of the distortion from a regular “icosahedral-like” shape, the carbon contributing to such a deformation to a lesser extent.

Table 1. Selected Geometrical Parameters at the RM2(fc)/6-31G* Level[a]

	2$^-$	**2**	**3**	**5**$^-$	**6**$^-$	**7**$^-$
			bond lengths (Å)			
1−2	1.772	1.753	1.782	1.767	1.767	1.779
1−3	1.755	1.769	1.760	1.757	1.767	1.753
1−4	1.748	1.771	1.756	1.767	1.767	1.753
1−5	1.784	1.762	1.767	1.785	1.784	1.779
1−6	1.803	1.796	1.788	1.785	1.775	1.796
2−3	1.838	1.817	1.818	1.835	1.818	1.816
2−6	1.767	1.778	1.741	1.753	1.773	1.768
3−4	1.831	1.824	1.839	1.835	1.776	1.786
4−5	1.772	1.765	1.823	1.753	1.751	1.816
5−6	1.744	1.758	1.768	1.765	1.824	1.768
2−7	2.040	2.012	2.033	2.035	2.051	2.048
2−11	1.823	1.831	1.839	1.838	1.808	1.820
3−7	2.102	2.073	2.095	2.093	2.048	2.056
3−8	2.086	2.091	2.069	2.093	1.726	1.724
4−8	2.035	2.031	2.067	2.035	1.699	1.724
4−9	1.737	1.722	2.094	1.838	1.775	2.056
5−9	1.703	1.678	2.032	1.775	1.833	2.048
5−10	1.787	1.800	1.724	1.697	2.044	1.820
6−10	1.790	1.800	1.699	1.697	2.050	1.768
6−11	1.766	1.777	1.779	1.775	1.804	1.768
7−8	2.210	2.229	2.246	2.252	1.891	1.885
8−9	1.878	1.879	2.219	1.953	1.621	1.885
9−10	1.631	1.656	1.876	1.626	1.965	1.945
10−11	1.737	1.834	1.622	1.626	1.980	1.751
7−11	1.959	2.042	1.958	1.953	1.945	1.945
mean B−H	1.197	1.190	1.190	1.197	1.197	1.197
C−H	1.091	1.089	1.091	1.090	1.090	1.090
B10−H_b	1.333					
B11−H_b	1.297					
			bond angles (deg)			
7−8−9	98.1	103.1	101.1	97.4	115.9	114.4
8−9−10	117.1	115.7	101.3	114.8	113.8	98.2
9−10−11	111.9	111.0	119.1	115.7	96.4	111.4
10−11−7	111.4	111.9	117.3	114.8	111.9	111.4
11−7−8	99.2	95.8	99.6	97.4	97.5	98.2
			dihedral angles (deg)			
7−8−9−10	10.5	15.5	11.0	1.2	−8.5	−25.2
9−8−7−11	−2.7	−7.5	−6.7	0.0	18.2	25.2

[a] For bond numbering, see Figure 1.

The “bridging” B10−B11 separation in **2** is ca. 0.01 Å longer than the corresponding length in **2**$^-$. The most

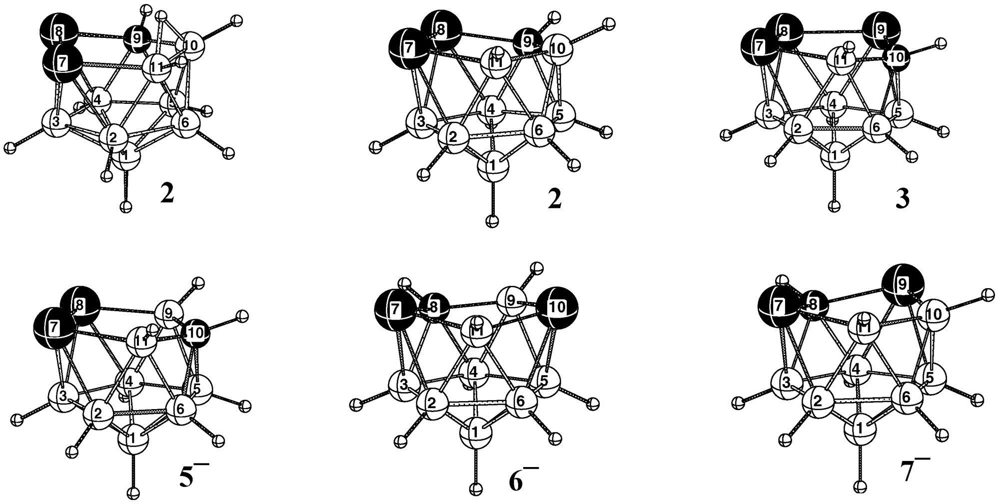

Figure 1. The structures of the eleven-vertex nido compounds 7,8,9-$P_2CB_8H_{10}$ (**2**), [7,8,9-$P_2CB_8H_9$]$^-$ (**2**$^-$), 7,8,9,10-$P_3CB_7H_8$ (**3**), [7,8,10-$P_2CB_8H_9$]$^-$ (**5**$^-$), [7,10,8-$P_2CB_8H_9$]$^-$ (**6**$^-$), and [7,9,8-$P_2CB_8H_9$]$^-$ (**7**$^-$) optimized at the RMP2(fc)/6-31G* level. ● = P, ● = C, ○ = B, and ○ = H.

Table 2. Calculated versus Experimental δ (^{11}B) and δ (^{13}C) NMR Shifts

	vertex number[a]									
compd	1	2	3	4	5	6	8	9	10	11
2	−26.0	16.5	−10.9	−7.5	18.2	−12.7		49.7	−9.6	−15.7
exp	−26.0	12.4	−12.7	−9.8	16.8	−12.7		58.7	−9.0	−15.8
2$^-$	−37.2	−9.2	−16.0	−9.6	−7.0	3.8		41.3	−1.1	−8.0
exp	−35.1	−11.1	−16.4	−11.1	−7.6	0.3		48.3	1.8	
3	−30.4	3.6	7.3	−5.8	4.5	9.3			52.6	2.6
exp	−28.6	3.3	5.5	−5.4	4.4	8.6			53.6	2.4
5$^-$	−36.2	−14.3	−2.1	−14.3	−1.7	−1.7		−5.9	41.4	−5.9
exp	−35.1	−14.6	−5.9	−14.6	−2.7	−2.7		−4.9	48.3	−4.9
6$^-$	−37.5	−14.4	−4.2	−8.7	−6.4	−1.7	33.6	−8.2		−12.3
7$^-$	−37.1	−14.3	−10.7	−10.7	−14.3	4.0	27.3		−8.1	−8.1

[a] For numbering, see Figure 1.

Table 3. Wiberg Bond Indices within the Open Pentagonal Face[a]

	bond				
	7−8	8−9	9−10	10−11	7−11
2	0.8626	0.7898	0.7483	0.4577	0.7333
3	0.7902	0.8605	0.7885	0.7883	0.8851
5$^-$	0.7723	0.8514	0.7777	0.7777	0.8514
6$^-$	0.7596	0.7866	0.8654	0.8201	0.8907
7$^-$	0.7502	0.7502	0.8912	0.7583	0.8912
2$^-$	0.8455	0.7876	0.7778	0.7900	0.8555

[a] For bond numbering, see Figure 1.

Table 4. Energy Data for Positional Isomers of [*nido*-$PC_2B_8H_9$]$^-$

isomer	symmetry	ZPE[a] (kcal mol^{-1})	RMP2/6-31G*[b] (Hartree)	relative energies[c] (kcal mol^{-1})
5$^-$ (7,8,10)	C_s	87.34795(0)	−923.2699196	0.000
6$^-$ (7,10,8)	C_1	87.37350(0)	−923.2665955	2.109
7$^-$ (7,9,8)	C_s	87.00876(0)	−923.2421746	17.108
2$^-$ (7,8,9)	C_1	86.91989(0)	−923.2405609	18.042

[a] Zero-point energies were calculated at the RHF/6-31G* level. The number of imaginary frequencies (NIMAG) is given in parentheses. [b] Total energies at the RMP2/6-31G* level. [c] Relative energies with ZPEs corrections scaled by 0.89.

remarkable features of the computed molecular structures of these systems consist of considerable deformations of the open-face pentagons. These distortions from the ideal pentagonal angle of 108° are best documented by the open-face P−P−B, P−P−C, P−C−B, and P−P−P angles in Table 1. Moreover, these pentagons are not planar, as exemplified by some dihedral angles in Table 1, although such a nonplanarity is less marked in the neutral species **2** and in anion **5**$^-$, in which the pentagonal belt in is almost planar. Internal coordinates associated with the open pentagonal belts resemble those determined for the four $P_2C_2B_7H_9$ isomers and their Cl-derivatives[6] at the same level of theory and approximate almost single-bond character, which is also in agreement with their Wiberg bond indices (see Table 3). Note that neither the Me nor Cl substitutions at B4 in **3**[7] affect the shape of the open pentagonal belt in **3** at all. Although just two positional isomers of [*nido*-$P_2CB_8H_9$]$^-$ have been prepared thus far, we have also investigated the remaining two structural alternatives (**6**$^-$ and **7**$^-$) computationally (see Tables 1−4). The calculations show that, of the four open-face isomers [*nido*-$P_2CB_8H_9$]$^-$, **5**$^-$ appears to be the most stable (see Table 4), which might be a consequence of essentially planar shape of the open pentagonal face (see Table 1). This observation is in accordance with the DFT and increment approaches.[12,13] These, however, show that **7**$^-$ should be the least stable isomer, which is slightly in contradiction with our calculations. Nevertheless, the energetic separation between **2**$^-$ and **7**$^-$ is predicted to be very small (see Table 4) by either of the methods mentioned. We might thus conclude that **2**$^-$ and **7**$^-$ exhibit about the same stability and are considerably less stable than **5**$^-$ and **6**$^-$.

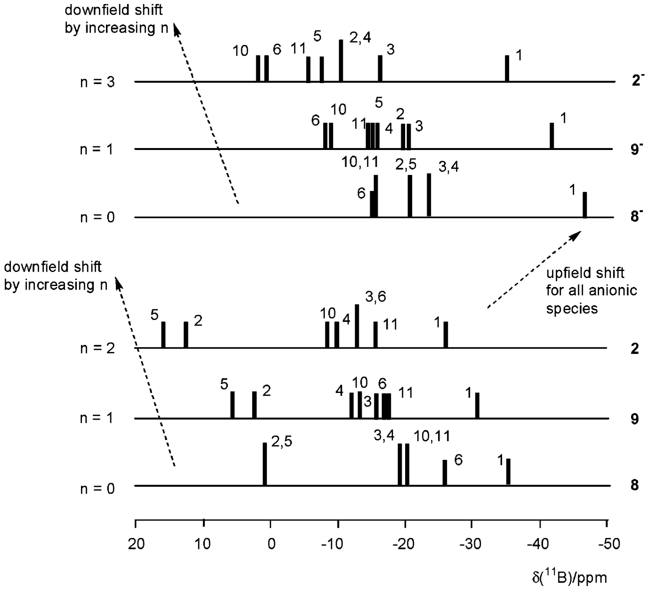

Figure 2. Simplified stick diagrams comparing the ^{11}B NMR chemical shifts and relative intensities for a series of isoelectronic eleven-vertex nido compounds with general formulas of 7,8,9-$P_nC_{3-n}B_8H_{12-n}$ (bottom traces) and [7,8,9-$P_nC_{3-n}B_8H_{11-n}$]$^-$ (upper traces) (data for compounds with n = 0 and 1 from refs 13 and 3, respectively).

NMR Studies. As shown by simplified stick diagrams in Figure 2, the ^{11}B NMR spectra of the asymmetrical compounds **2** and **2**$^-$ consist of eight different doublet resonances with some incidental overlaps. It is also obvious that the ^{11}B NMR signals of the anionic compound **2**$^-$ are shifted to lower frequencies in comparison to those of the neutral compound **2**. Figure 2 also shows graphical comparisons of the ^{11}B NMR shifts for **2** and for the isostructural nido compounds 7,8,9-$C_3B_8H_{12}$ (**8**)[10,14] and 7,8,9-$PC_2B_8H_{11}$ (**9**)[4] (bottom diagrams) together with similar relationships for the corresponding anionic species [7,8,9-$C_3B_8H_{11}$]$^-$ (**8**$^-$),[10,14] [7,8,9-$PC_2B_8H_{10}$]$^-$ (**9**$^-$),[4] and **2**$^-$ (upper diagrams). These graphics demonstrate that the δ (^{11}B) data for a series of isostructural compounds of general formulations 7,8,9-$P_nC_{3-n}B_8H_{12-n}$ (bottom traces) and [7,8,9-$P_nC_{3-n}B_8H_{11-n}$]$^-$ (upper traces) are very similar and that a formal replacement of one CH unit with the isolobal P-vertex causes a systematic high-frequency shift by an increment of $\Delta\delta = \sim 5$ ppm. The ^{11}B NMR spectrum of the triphosphacarborane **3** contains seven different doublet resonances, while the spectrum of anion **5**$^-$, C_s symmetry, consists of 2:2:1:2:1 patterns of doublets. Figure 3 (bottom traces) shows straightforward NMR similarities between **5**$^-$ and its isostructural counterpart [7,8,-

---

(11) Bühl, M.; Schleyer, P. v. R. *J. Am. Chem. Soc.* **1992**, *114*, 477.

(12) Hofmann, M.; Fox, M. A.; Greatrex, R.; Schleyer, P. v. R.; Williams, R. E. *Inorg. Chem.* **2001**, *40*, 1790.

(13) Farooq, K. A.; Hofmann, M. *Inorg. Chem.* **2005**, *44*, 3746.

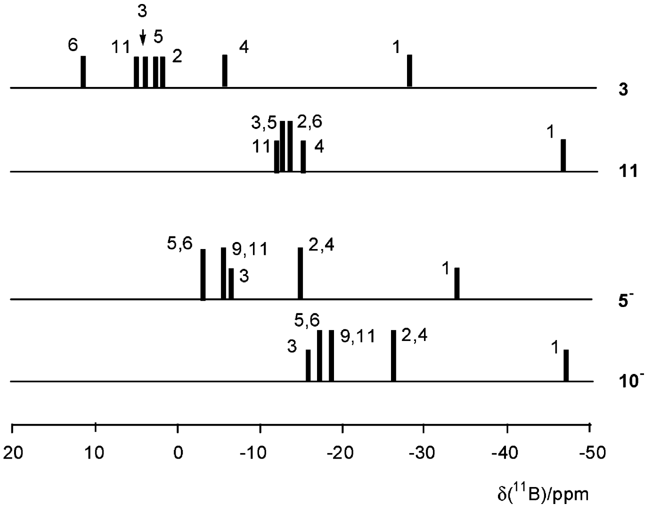

Figure 3. Simplified stick diagrams comparing the ^{11}B NMR chemical shifts and relative intensities for eleven-vertex nido compounds $[7,8,10\text{-}C_3B_8H_{11}]^-$ (**10**$^-$) (data from ref 10) and $[7,8,10\text{-}P_2CB_8H_9]^-$ (**5**$^-$) (bottom traces) together with those for $7,8,9,10\text{-}C_4B_7H_{11}$ (**11**) (data from ref 15) and $7,8,9,10\text{-}P_3CB_7H_8$ (**3**) (upper traces).

$10\text{-}C_3B_8H_{11}]^-$ (**10**$^-$).[10]In this case, the ^{11}B NMR signals of **5**$^-$ are again shifted to high frequencies by the increment of $\Delta\delta = \sim 10$ ppm; this is the result of the isolobal replacement of two CH vertexes with P units.

Figure 3 (upper traces) also shows the ^{11}B NMR relationship between the triphosphacarborane **3** and the isoelectronic tetracarbaborane *nido*-$7,8,9,10\text{-}C_4B_7H_{11}$ (**11**).[15] The diagram shows that isolobal replacement of three CH vertexes with P in **11** causes a high-frequency shift of the whole spectrum of **3** by an increment of $\Delta\delta = \sim 15$ ppm.

The characteristic feature of the ^1H NMR spectra of compounds **2**, **2**$^-$, and **3** is the presence of one CH doublet (^2J(P,H) coupling because of the cage CH unit adjacent to the P-vertex), while the spectrum of **5**$^-$ shows a singlet CH resonance. The spectrum of the neutral compound **2** contains a typical broad, high-field μH(10,11) resonance at -2.36 ppm. The ^{31}P NMR spectra of compounds **2** and **2**$^-$ exhibit two signals split into asymmetric doublets because of ^1J(P,P), while the spectrum of **3** consists of two asymmetric doublets (assigned to P7 and P9) and one asymmetric triplet from the P8 resonance. In accordance with the C_s symmetry, the ^{31}P NMR spectrum of **5**$^-$ contains only one singlet. The severely broadened ^{13}C NMR signals of some of the phosphacarborane compounds discussed above could be measured by gradient-enhanced [$^1H-^{13}C$] HSQC experiments[16] (Figure 4) even with surprisingly small amounts of the sample.

Because the ^1H (cage CH) NMR signals are also broadened, their magnetization is rapidly lost in the course of the pulse sequence when the incremented delays become longer. It is therefore advisable to use a greater number of transients and take the first 16 or 32 of typically 256 experiments for the Fourier transformation. The tilt of the cross-peaks[17] in these 2D NMR experiments reveal that the signs of the coupling constants, $^1J(^{31}P,^{13}C)$ and $^2J(^{31}P,^1H)$, are opposite. There are promising aspects of calculating coupling constants by DFT methods if the molecular geometries have been optimized using a sufficiently large basis set,[18] which has also been demonstrated for boron compounds.[19] We have now applied such calculations at the B3LYP/6-311+G(d,p) level of theory to compounds **2**, **3**, and **2**$^-$, for all of which the 2D $^1H-^{13}C$ experiments have been carried out successfully. Table 5 shows that the agreement between calculated and experimental data is reasonable, and it appears that the correct signs of the coupling constants may be predicted. The negative sign of $^1J(^{31}P,^{13}C)$ is expected to result from the effects of the lone electron pair on the phosphorus atom.[20] This also applies to the positive sign of $^2J(^{31}P,C,^1H)$, considering the assumed syn orientation of the phosphorus lone pair and the C−H bond vector. This discussion also includes the magnitude and sign of the coupling constants $^1J(^{31}P,^{31}P)$. The negative sign of $^1J(^{31}P,^{31}P)$ is in full agreement with the influence of the lone pairs of electrons on the phosphorus atoms, and agrees with the experimental findings for some other phosphapolyboranes.[22] It should be noted that the calculated contribution of the paramagnetic spin−orbital term to $^1J(^{31}P,^{31}P)$ is fairly large and negative [e.g., -82.9 Hz in **2** or -71.4 Hz (8,9) and -54.0 Hz (7,8) in **3**]. This contribution is also noteworthy for $^1J(^{31}P,^{13}C)$ (e.g., -13.5 Hz in **2** or -12.0 Hz in **3**). However, the Fermi contact term is still the dominating coupling mechanism.

Conclusions

We have demonstrated that, under the reaction conditions employed, phosphorus insertion into the now readily available carborane $4\text{-}CB_8H_{14}$ (**1**)[23] leads mainly to the neutral compound $7,8,9\text{-}P_2CB_8H_{10}$ (**2**) and that the reaction is accompanied by the formation of smaller amounts of $7,8,9,10\text{-}P_3CB_7H_8$ (**3**) and $2,1\text{-}P_2CB_8H_{10}$ (**4**). Deprotonation of **2** generates a bare pentagonal face belonging to the $[7,8,9\text{-}P_2CB_8H_9]^-$ (**2**$^-$) anion, which can be thermally rearranged into its symmetrical $[7,8,10\text{-}P_2CB_8H_9]^-$ (**5**$^-$) isomer. This chem-

---

(14) Štíbr, B.; Holub, J.; Teixidor, F.; Viñas, C. *J. Chem. Soc. Chem. Commun.* **1995**, 795.

(15) Štíbr, B.; Jelínek, T.; Drdáková, E.; Heømánek, S.; Plešek, J. *Polyhedron* **1988**, *7*, 669.

(16) Kontaxis, G.; Stonehouse, J.; Laue, E. D.; Keeler, J. *J. Magn. Reson., Ser. A* **1994**, *111*, 70.

(17) Bax, A.; Freeman, R. *J. Magn. Reson.* **1981**, *45*, 177.

(18) (a) Sychrovsky, V.; Gräfenstein, J.; Cremer, D. *J. Chem. Phys.* **2000**, *113*, 3530. (b) Wu, A.; Gräfenstein, J.; Cremer, D. *J. Phys. Chem.* A **2003**, *107*, 7043. (c) Barone, V.; Peralta, J. E.; Contreras, R. H.; Snyder, J. P. *J. Phys. Chem.* A **2002**, *106*, 5607. (d) Krivdin, L. B.; Sauer, S. P. A.; Peralta, J. E.; Contreras, R. H. *Magn. Reson. Chem.* **2002**, *40*, 187. (e) Peralta, J. E.; Scuseria, G. E.; Cheeseman, J. R.; Frisch, M. J. *Chem. Phys. Lett.* **2003**, *375*, 452. (g) Helgaker, T.; Jaszinski, M.; Ruud, K.; Gorska, A. *Theor. Chem. Acct.* **1998**, *99*, 175.

(19) (a) Onak, T.; Jaballas, J.; Barfield, M. *J. Am. Chem. Soc.* **1999**, *121*, 2850. (b) Wrackmeyer, B.; Berndt, A. *Magn. Reson. Chem.* **2004**, *42*, 490.

(20) Gil, V. M. S.; von Philipsborn, W. *Magn. Reson. Chem.* **1989**, *27*, 409.

(21) Van Wüllen, C. *Phys. Chem. Chem. Phys.* **2000**, *2*, 2137.

(22) Keller, W.; Haubold, W.; Wrackmeyer, B. *Magn. Reson. Chem.* **1999**, *37*, 545.

(23) (a) Jelínek, T.; Štíbr, B.; Holub, J.; Bakardjiev, M.; Hnyk, D.; Ormsby, D. L.; Killner, C. A.; Thornton-Pett, M.; Schanz, H.-J.; Wrackmeyer, B.; Kennedy, J. D. *Chem. Commun.* **2001**, 1756. (b) Brellochs, B.; Bačkovský, J.; Štíbr, B.; Jelínek, T.; Holub, J.; Bakardjiev, M.; Hnyk, D.; Hofmann, M.; Císařová, I.; Wrackmeyer, B. *Eur. J. Inorg. Chem.* **2004**, 3605.

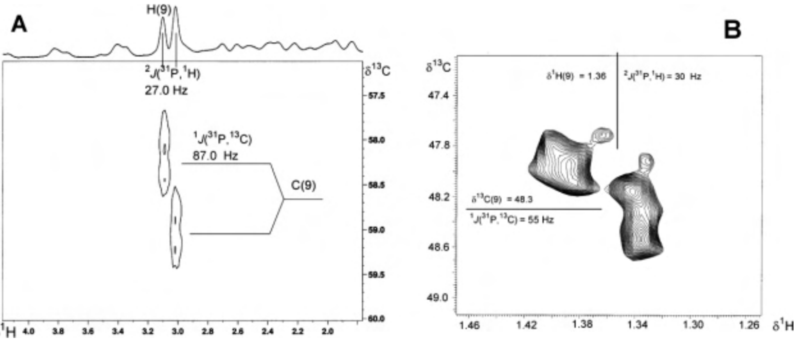

Figure 4. (A) Contour plot of the 100.6 MHz gradient-enhanced [$^1H-^{13}C$] HSQC experiment for **2** in CD_2Cl_2 (8 mg in 0.5 mL, total measuring time 2 h), showing the cross-peak for the $^{13}C(9)$ NMR signal. The coupling constant $^1J(^{31}P,^{13}C)$ is clearly resolved, whereas the information on $^2J(^{31}P,^{13}C)$ is not well resolved because of the broadening by partially relaxed $^{13}C-^{11}B$ spin−spin coupling. The doublet splitting shows a negative tilt which indicates that the signs of $^1J(^{31}P,^{13}C)$ and $^2J(^{31}P,^1H)$ are opposite. (B) Contour plot of the 125.8 MHz gradient-enhanced [$^1H-^{13}C$] HSQC experiment for the anion **2**$^-$ dissolved as the Ph_4P^+ salt in CD_2Cl_2 (0.8 mg in 0.5 mL, recorded using a cryo probe with a total measuring time of 4 h). The doublet splittings from $^1J(^{31}P,^{13}C)$ and $^2J(^{31}P,^1H)$ show a negative tilt, which indicates that the signs of these coupling constants are opposite.

Table 5. Some Experimental and Calculated Coupling Constants (in Hz) and ^{13}C and ^{31}P Chemical Shifts (in ppm) for the Eleven-Vertex nido Compounds 7,8,9-$P_2CB_8H_{10}$ (**2**), 7,8,9,10-$P_3CB_7H_8$ (**3**), and [7,8,9-$P_2CB_8H_9$]$^-$ (**2**$^-$)

	2	3	2$^-$
$^1J(^{31}P,^{13}C)_{exp}$	87.0	92.6	55.0
$^1J(^{31}P,^{13}C)_{calcd}$	−104.0	−96.9	−82.8
$^2J(^{31}P,C,^1H)_{exp}$	27.0	30.0	30.0
$^2J(^{31}P,C,^1H)_{calcd}$	36.7	38.5	36.0
$^1J(^{31}P,^{31}P)_{exp}$	267.0	261.0, 209.0[a]	206.0
$^1J(^{31}P,^{31}P)_{calcd}$	−278.8	−255.1, −226.6[a]	−255.3
$\delta\ (^{13}C)_{exp}$	58.7	62.2	48.3
$\delta\ (^{13}C)_{calcd}$[b]	66.1	70.9	55.7
$\delta\ (^{31}P)_{calcd}$[c]	11.8, 44.8	35.6, 20.8, 50.5[d]	−42.5, −58.7[e]-
$\delta\ (^{31}P)_{exp}$	−25.5, 15.6	−7.6, −26.7, 24.8[d]	25.5, −76.5[e]

[a] For P8,9 and P7,8, respectively. [b] $\delta\ (^{13}C)_{calcd} = \sigma\ (^{13}C)(Me_4Si) - \sigma\ (^{13}C)$, for $\sigma\ (^{13}C)(Me_4Si) = 184.0$. [c] The choice of a correct reference for $\sigma\ (^{31}P)$ values is a problem: the trend of calculated $\sigma\ (^{31}P)$ values is in good agreement with the experimental $\delta\ (^{31}P)$ data. Calculated $\sigma\ (^{31}P)$ data are converted to $\delta^{31}P$ data by $\delta\ (^{31}P)_{calcd} = \sigma\ (^{31}P)\ (PH_3) - \sigma\ (^{31}P) - 266.1$, with $\sigma\ (^{31}P)\ (PH_3) = +563.2$, $\delta\ (^{31}P)\ (PH_3) = -266.1$, and $\delta\ (^{31}P)\ (H_3PO_4$, aq, 85%) = 0.[21] [d] For P7, P8, and P9, respectively. [e] For P7 and P8, respectively.

istry of **2** is entirely analogous to that of the neutral tricarbollide 7,8,9-$C_3B_8H_{12}$ (**8**),[10,14] which also reflects the isolobal relationship between the bare P vertex and the cage CH group. It should be also pointed out that all eleven-vertex nido compounds isolated in this study exhibit extreme air stability and are thus useful for further syntheses in the area of phosphacarborane chemistry. Moreover, anionic compounds **2**$^-$ and **5**$^-$ are straightforward analogues of the Cp anion as they are monoanionic, contain a bare pentagonal face, and would then be capable of donating five electrons for the η^5-type complexation of suitable metal centers. Relevant extensions of this type of metalladiphosphacarborane chemistry are being in progress in our laboratories.

Experimental Section

Material and Methods. All reactions were carried out with use of standard vacuum or inert-atmosphere techniques as described by Shriver,[24] although some operations, such as column LC, were carried out in air. The starting carborane, **1**, was prepared according to the literature.[23] The Fluka dichloromethane and hexane were dried over CaH_2 and freshly distilled before use. Other chemicals were reagent or analytical grade and were used as purchased. Column chromatography was carried out using silica gel (Aldrich, 130−270 mesh) as the stationary phase. The purity of individual chromatographic fractions was checked by analytical TLC on Silufol (silica gel on aluminum foil, detection by diiodine vapor, followed by 2% aqueous $AgNO_3$ spray). Melting points were measured in sealed capillaries under argon and are uncorrected. Mass spectrometry and NMR spectroscopy were performed as described earlier by our groups.[4] Because of the broadening of the ^{13}C(carborane) NMR signal caused by the partially relaxed scalar $^1J(^{13}C,^{11}B)$ and $^1J(^{13}C,^{31}P)$ spin−spin couplings, the ^{13}C(cage) NMR signals could not be observed by direct measurements. The best results were obtained using the gradient-enhanced [$^1H-^{13}C$] HSQC pulse sequence.[16] Measurements were carried out on Bruker Avance 400 (compounds **2** and **3**) and Avance 500 (with a cryo probe, for **2**$^-$) instruments.

Preparation of *nido*-7,8,9-$P_2CB_8H_{10}$ (2) and *nido*-7,8,9,10-$P_3CB_7H_8$ (3). A solution of compound **1** (500 mg, 4.44 mmol) in CH_2Cl_2 (25 mL) was added dropwise over a period of 2 h to a solution containing PCl_3 (1.923 g, 14 mmol) and PS (3.22 g, 15 mmol) in CH_2Cl_2 (25 mL) while the mixture was stirred and cooled to 0 °C. The mixture was then stirred for 24 h at ambient temperature, cooled again to 0 °C, and decomposed carefully with water (50 mL) under intensive stirring. The CH_2Cl_2 layer was separated; the solvent was evaporated, and the residual materials were separated via chromatography in hexane on a silica gel column (30 × 2.5 cm) to collect pure fractions of R_f (hexane) = 0.73, 0.60, and 0.40. The fractions were evaporated and the solid residues sublimated in vacuo to obtain compounds **3** (42 mg, 5%), **4** (92 mg, 15%, for characterization see reference[8]), and **2** (257 mg, 34%), respectively.

Compound 2. R_f (hexane): 0.40. mp: 190 °C. ^{11}B NMR (160.3 MHz, $CDCl_3$, 295 K): δ 16.8 (d, $^1J(B,H) = 165$ Hz, 1 B, B5), 12.4 (d, $^1J(B,H) = 166$ Hz, 1 B, B2), −9.0 (d, $^1J(B,H) = \sim 140$ Hz, $^1J(B,\mu H) = 38$ Hz, 1 B, B10), −9.8 (d, $^1J(B,H) = \sim 130$ Hz, 1 B, B4), −12.7 (d, $^1J(B,H) = \sim 160$ Hz, 2 B, B3,6), −15.8 (d, $^1J(B,H) = 154$ Hz, 1 B, B11), −26.0 (d, $^1J(B,H) = 158$ Hz, 1 B, B1). All of the expected [^{11}B-^{11}B]-COSY cross-peaks were observed, except for B5−B10. $^1H\{^{11}B\}$NMR (500 MHz, $CDCl_3$, 295 K): δ 3.57 (s, 1 H, H5), 3.50 (d, $^2J(P,H) = 25$ Hz, 1 H, H2), 2.95 (d, $^2J(P,H) = 27$ Hz, 1 H, H9), 2.70 (d, $^2J(P,H) = 18$ Hz, 1 H, H4), 2.56 (s, 1 H, H10), 2.43 (s, 1 H, H1), 2.20 (d, $^2J(P,H) = 7$ Hz, 1 H, H2), 2.15 (s, 1 H, H5), −2.36 (s, 1 H, μH10,11). ^{13}C NMR (100.6 MHz, CD_2Cl_2, 295 K): δ 58.7 (d, $^1J(P,C) = 87$ Hz, 1 C, C9) (determined by gradient-enhanced [$^1H-^{13}C$] HSQC measurements). $^{31}P\{^1H\}$ NMR (202.3 MHz, $CDCl_3$, 295 K): δ 15.6 (asym.d, $^1J(P,P) = 267$ Hz, 1 P, P8), −25.5 (d, $^1J(P,P) = 267$ Hz, 1 P, P7) (assigned by $^1H\{^{31}P$(selective)$\}$ measurements). MS (70 eV, EI): m/z 172(15) $[M]^+$, 169(100) $[M - 3H]^+$. Anal. Calcd for $CH_{10}B_8P_2$ (170.52): C, 7.04; H, 5.91. Found: C, 7.24; H, 6.12.

Compound 3. R_f (hexane): 0.73. mp: 182 °C. ^{11}B NMR (160.3 MHz, $CDCl_3$, 295 K): δ 8.6 (d, $^{1}J(B,H) = 158$ Hz, 1 B, B6), 5.5 (d, $^{1}J(B,H) = \sim150$ Hz, 1 B, B11), 4.4 (d, $^{1}J(B,H) = \sim180$ Hz, 1 B, B3), 3.3 (d, $^{1}J(B,H) = \sim170$ Hz, 1 B, B5), 2.4 (d, $^{1}J(B,H) = \sim150$ Hz, 1 B, B2), -5.4 (d, $^{1}J(B,H) = 162$ Hz, 1 B, B4), -28.6 (d, $^{1}J(B,H) = 154$ Hz, 1 B, B1). All of the expected $[^{11}B\text{-}^{11}B]$-COSY cross-peaks were observed. $^{1}H\{^{11}B\}$NMR (500 MHz, $CDCl_3$, 295 K): δ 3.20 (s, 1 H, H6), 3.50 (t, $^{2}J(P,H) = 25$ Hz, 1 H, H3), 3.18 (d, $^{2}J(P,H) = 15$ Hz, 1 H, H5), 3.13 (s, 1 H, H11), 2.89 (d, $^{2}J(P,H) = 25$ Hz, 1 H, H2), 2.81 (d, $^{2}J(P,H) = 30$ Hz, 1 H, H10), 2.77 (s, 1 H, H1). ^{13}C NMR (100.6 MHz, CD_2Cl_2, 295 K): δ 62.2 (d, $^{1}J(P,C) = 92.6$ Hz, Hz, 1 C, C9) (determined by gradient-enhanced $[^{1}H-^{13}C]$ HSQC measurements). $^{31}P\{^{1}H\}$ NMR (202.3 MHz, $CDCl_3$, 295 K): δ 24.8 (asym.d, $^{1}J(P,P) = 261$ Hz, 1 P, P9), -7.6 (asym.d, $^{1}J(P,P) = 209$ Hz, 1 P, P7), -26.7 (asym.t, $^{1}J(P,P) = 208/265$ Hz, 1 P, P8) (assigned by $^{1}H\{^{31}P(\text{selective})\}$ measurements). MS (70 eV, EI): m/z 190(16) $[M]^+$, 187(100) $[M - 3H]^+$. Anal. Calcd for $CH_8B_7P_3$ (188.67): C, 6.37; H, 4.27. Found: C, 6.51; H 4.48.

Preparation of the [*nido*-7,8,9-$P_2CB_8H_9$]$^-$ Anion (2^-). ($PPh_4^+2^-$). A suspension of NaH (50 mg, 2.0 mmol) in Et_2O (20 mL) was treated with a solution of compound **2** (171 mg, 1 mmol) under stirring at room temperature for 2 h (hydrogen evolution). The mixture was filtered; the filtrate was evaporated, and the residue was dried in vacuo. The residual solid was dissolved in water (20 mL), and the solution precipitated with 0.1 M aqueous PPh_4Cl (10 mL). The white solid was isolated by filtration, dried in vacuo for 6 h, and crystallized by diffusion of hexane vapors into a CH_2Cl_2 solution to isolate 473 mg (93%) of $PPh_4^+\mathbf{2}^-$. R_f (CH_2Cl_2): 0.10. mp: 270 °C. ^{11}B NMR (160.3 MHz, CD_3CN, 295 K): δ 1.8 (br. s, $^{1}J(B,B) = \sim35$ Hz, 1 B, B10), 0.3 (d, $^{1}J(B,H) = 131$ Hz, 1 B, B6), -6.1 (br. s, complex $^{1}J(B,B)$ and $^{1}J(B,P)$ splitting, 1 B, B11), -7.6 (d, $^{1}J(B,H) = 150$ Hz, 1 B, B5), -11.1 (d, $^{1}J(B,H) = \sim155$ Hz, 2 B, B2,4), -16.4 (d, $^{1}J(B,H) = 165$ Hz, 1 B, B3), -35.1 (d, $^{1}J(B,H) = 158$ Hz, 1 B, B1). All of the expected $[^{11}B\text{-}^{11}B]$-COSY cross-peaks were observed, except for B5−B10. $^{1}H\{^{11}B\}$NMR (500 MHz, CD_3CN, 295 K): δ 2.57 (s, 1 H, H10), 2.52 (d, $^{2}J(P,H) = 15$ Hz, 1 H, H2 or H4), 2.13 (t, $^{2}J(P,H) = 14$ Hz, 1 H, H3), 2.06 (s, 1 H, H5), 1.63 (d, $^{2}J(P,H) = 17$ Hz, 1 H, H2 or H4), 1.56 (d, $^{2}J(P,H) = 32$ Hz, 1 H, H11), 1.47 (s, 1 H, H1), 1.29 (d, $^{2}J(P,H) = 30$ Hz, 1 H, H9). ^{13}C NMR (125.8 MHz, CD_2Cl_2, 295 K): δ 48.3 (d, $^{1}J(P,C) = 55$ Hz, 1 C, C9) (determined by $[^{1}H-^{13}C]$ HSQC measurements). $^{31}P\{^{1}H\}$ NMR (202.3 MHz, CD_3CN, 295 K): δ -76.5 (asym.d, $^{1}J(P,P) = 206$ Hz, 1 P, P8), -25.5 (d, $^{1}J(P,P) = 206$ Hz, 1 P, P7) (assigned by $^{1}H\{^{31}P(\text{selective})\}$ measurements). Anal. Calcd (%) for $C_{25}H_{29}B_8P_3$ (508.95): C, 58.99; H, 5.74. Found: C, 57.12; H, 5.89.

(PSH^+2^-). PS (193 mg, 0.9 mmol) was added to a solution of **2** (129 mg, 0.85 mmol) in CH_2Cl_2 (10 mL) while it was stirred and cooled to 0 °C. A layer of hexane (20 mL) was then carefully added onto the surface of the solution, and the mixture was left to crystallize for 48 h. The colorless crystals were then isolated by filtration, washed with hexane, and vacuum-dried at room temperature to give $PSH^+\mathbf{2}^-$ (290 mg, 92%). The crystallization of an analytical sample was achieved by diffusion of pentane vapors into a CH_2Cl_2 solution. The ^{11}B NMR spectrum of was nearly identical to that of $PPh_4^+\mathbf{2}^-$.

Preparation of PPh_4^+[*nido*-7,8,10-$P_2CB_8H_9$]$^-$ ($PPh_4^+5^-$). A suspension of NaH (50 mg, 2.0 mmol) in Et_2O (20 mL) was treated with a solution of compound **2** (171 mg, 1.0 mmol) under stirring at room temperature for 2 h (hydrogen evolution). The mixture was filtered; the filtrate was evaporated, and the residue was dried in vacuo. The residual solid was then heated under argon at 350 °C for 2 h. The residual solid was dissolved in water (20 mL), and the solution was precipitated with solid PPh_4Cl (400 mg, 1.1 mmol). The white solid was isolated by filtration, dried in vacuo for 6 h, and crystallized by diffusion of hexane vapors into a CH_2Cl_2 solution to isolate 438 mg, (86%) of $PPh_4^+\mathbf{5}^-$. R_f (CH_2Cl_2): 0.11. mp: 290 °C. ^{11}B NMR (160.3 MHz, CD_3CN, 295 K): δ -2.7 (d, $^{1}J(B,H) = 150$ Hz, 2 B, B5,6), -4.9 (d, $^{1}J(B,H) = 134$ Hz, 2 B, B9,11), -5.9 (br. s, $^{1}J(B,H) = \sim180$ Hz, 1 B, B3), -14.6 (d, $^{1}J(B,H) = 147$ Hz, 2 B, B2,4), -35.1 (d, $^{1}J(B,H) = 150$ Hz, 1 B, B1). All of the expected $[^{11}B-^{11}B]$ COSY cross-peaks were observed. $^{1}H\{^{11}B\}$NMR (500 MHz, CD_3CN, 295 K): δ 2.56 (t, $^{2}J(P,H) = 15$ Hz, 1 H, H3), 2.28 (s, 2 H, H5,6), 2.15 (s, 1 H, H10), 1.97 (d, $^{2}J(P,H) = \sim20$ Hz, 2 H, H9,11), 1.74 (br.s, 2 H, H2,4), 1.36 (s, 1 H, H1). $^{13}C\{^{1}H\}$ NMR (100.6 MHz, CD_3CN, 295 K): δ 53.6 (br.s, 1 C, C10). $^{31}P\{^{1}H\}$ NMR (202.3 MHz, CD_3CN, 295 K): δ -112.2 (s, 2 P, P7,8). Anal. calcd for $C_{25}H_{29}B_8P_3$ (508.95): C, 58.99; H, 5.74. Found: C, 56.94; H 5.61.

Computational Details. For the geometry optimizations (RHF/6-31G*, then RMP2(fc)/6-31G* as the final level of optimization) and frequency calculations (RHF/6-31G*, also the zero-point energies (ZPE)), we employed the standard ab initio methods[25] incorporated in the Gaussian 03 suite of programs.[26] They were performed on a FujitsuSiemens PC with this software. This program package also enabled us to compute both the Wiberg bond indices (WBI)[27] and the chemical shifts, the latter being calculated at a SCF level using the GIAO (gauge-invariant atomic orbital) method and employing a II Huzinaga basis set,[28] well-proven for the calculations of shielding tensors.[29] Coupling constants were calculated using the PC version of the Gaussian 03 program package.

Acknowledgment. This work was supported by Alexander von Humboldt Stiftung (FRG) (B. Š.), Deutsche Forschungsgemeinschaft (B. W.) and the Grant Agency of the Czech Republic (Grant 203/05/2646). We also thank Dr. Z. Plzák for help with the mass spectra, and Bruker for the ^{13}C NMR measurements with a cryo probe.

Supporting Information Available: Computed RMP2(fc)/6-31G* coordinates for compounds **2**, **2**$^-$, **3**, **5**$^-$, **6**$^-$, and **7**$^-$. This material is available free of charge via the Internet at http://pubs.acs.org.

IC048232C

---

(24) Shriver, D. F.; Drezdon, M. A. *Manipulation of Air-Sensitive Compounds*, 2nd ed.; Wiley: New York, 1986.

(25) Hehre, W.; Radom, L.; Schleyer, P. v. R.; Pople, J. A. *Ab initio Molecular Orbital Theory;* Wiley: New York, 1986.

(26) Frisch, M. J.; Trucks, G. W.; Schlegel, H. B.; Scuseria, G. E.; Robb, M. A.; Cheeseman, J. R.; Montgomery, J. A., Jr.; Vreven, T.; Kudin, K. N.; Burant, J. C.; Millam, J. M.; Iyengar, S. S.; Tomasi, J.; Barone, V.; Mennucci, B.; Cossi, M.; Scalmani, G.; Rega, N.; Petersson, G. A.; Nakatsuji, H.; Hada, M.; Ehara, M.; Toyota, K.; Fukuda, R.; Hasegawa, J.; Ishida, M.; Nakajima, T.; Honda, Y.; Kitao, O.; Nakai, H.; Klene, M.; Li, X.; Knox, J. E.; Hratchian, H. P.; Cross, J. B.; Adamo, C.; Jaramillo, J.; Gomperts, R.; Stratmann, R. E.; Yazyev, O.; Austin, A. J.; Cammi, R.; Pomelli, C.; Ochterski, J. W.; Ayala, P. Y.; Morokuma, K.; Voth, G. A.; Salvador, P.; Dannenberg, J. J.; Zakrzewski, V. G.; Dapprich, S.; Daniels, A. D.; Strain, M. C.; Farkas, O.; Malick, D. K.; Rabuck, A. D.; Raghavachari, K.; Foresman, J. B.; Ortiz, J. V.; Cui, Q.; Baboul, A. G.; Clifford, S.; Cioslowski, J.; Stefanov, B. B.; Liu, G.; Liashenko, A.; Piskorz, P.; Komaromi, I.; Martin, R. L.; Fox, D. J.; Keith, T.; Al-Laham, M. A.; Peng, C. Y.; Nanayakkara, A.; Challacombe, M.; Gill, P. M. W.; Johnson, B.; Chen, W.; Wong, M. W.; Gonzalez C.; Pople, J. A. *Gaussian 03*, revision B.03; Gaussian Inc.: Pittsburgh, PA, 2003

(27) Wiberg, K. *Tetrahedron* **1968**, *24*, 325.

(28) Huzinaga, S. *Approximate Atomic Wave Functions*; University of Alberta: Edmonton, Canada, 1971.

(29) Kutzelnigg, S. W.; Schindler, M.; Fleischer, U. *NMR, Basic Principles and Progress*; Springer: Berlin, New York, 1990; Vol. 23.